Minimal Solvers for Single-View Lens-Distorted Camera Auto-Calibration
Supplemental Material

A. Geometry of Input Features

As discussed in Sec. 5.1, the input configurations of the solvers provide extra measurements that can be used to reject invalid solutions. Circular arcs provide contour points that can be tested against the vanishing point. Region correspondences provide point correspondences in three other translational directions that can be tested against the vanishing lines. In the following sections, we discuss the construction of the circles and vanishing points.

A.1. Circle through Vanishing Point

The construction of the consistency measure (12) is a generalization of the Tardif consistency measure for vanishing points and imaged parallel lines introduced in [28]. Vanishing point $\mathbf{u}$ is recovered from a minimal solution. The join $\mathbf{m}$ of $\mathbf{u}$ with the undistorted midpoint $\overline{\mathbf{x}}$ of either the circular arc or the point correspondence is constructed (see the right part of Fig. A.1). Line $\mathbf{m}$ is distorted to a circle $\tilde{\mathbf{m}}$ using the minimal solution of the division model parameter, and the mean squared distances of image points to the circle $d_{\tilde{\mathbf{m}}}(\tilde{\mathbf{x}}_i)$ is computed (see the left part of Fig. A.1).

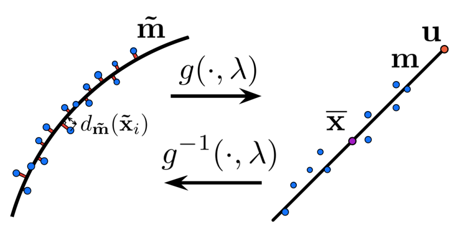

Figure A.1: *Geometry of the Consistency Measure.* Left is the distorted space, and right is the undistorted space. Midpoint $\overline{\mathbf{x}}$ and line $\mathbf{m}$ is constructed in undistorted space and then warped to distorted space. Mean-squared distance from the points to $\tilde{\mathbf{m}}$ is computed in the distorted space.

A.2. Vanishing Points from a Region Correspondence

Fig. A.2 shows two corresponded affine-covariant regions in two spaces: scene space and undistorted image space. In particular, affine-covariant regions are parameterized by affine frames (defined by three points), which is a common parameterization. Six point correspondences can be extracted from the region correspondence. The orientations of the joins of points are color coded.

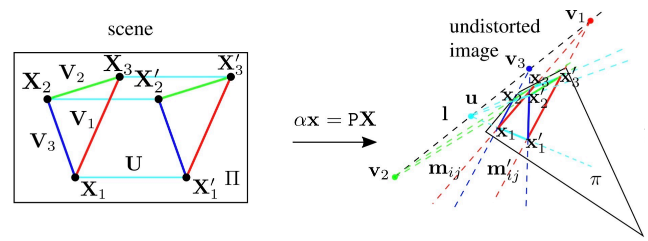

Figure A.2: *Geometry of an Affine-Covariant Region.* The scene plane Π contains the preimage of radially-distorted conjugately-translated affine-covariant regions, equivalently, 3 translated points in the direction $\mathbf{U}$. This configuration had 3 additional translation directions $\mathbf{V}_1$,$\mathbf{V}_2$,$\mathbf{V}_3$ that can be used to design a solver or to validate a minimal solution. Courtesy of [21].

Four vanishing points can be constructed from the red, green, blue and cyan lines. Up to two vanishing points are constructed by the solvers **4PC+2CA** and **2PC+4CA**. The remaining vanishing points can be estimated by constraining them to lie on the recovered vanishing line $\mathbf{l}$. Then the vanishing points can be used to validate the minimal solution of the division model parameter λ and $\mathbf{l}$ using the consistency measure (12).

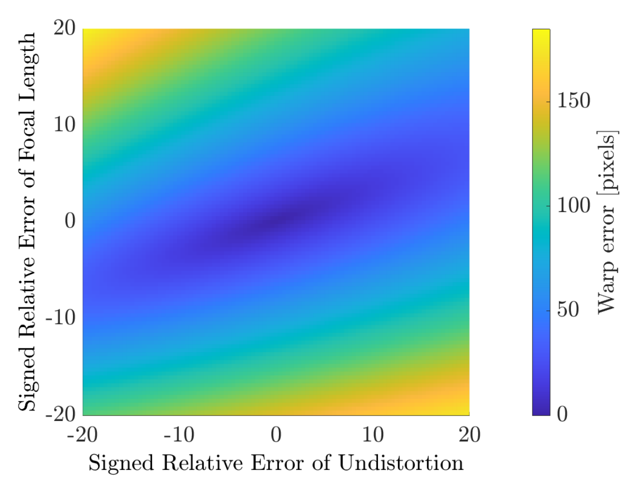

Figure A.3: *Warp Error as a Function of the Relative Errors of Undistortion and Focal Length.* The warp error is calculated for 100×100 tessellation of $[-20, 20] \times [-20, 20]$ space of the relative errors of undistortion and focal length.

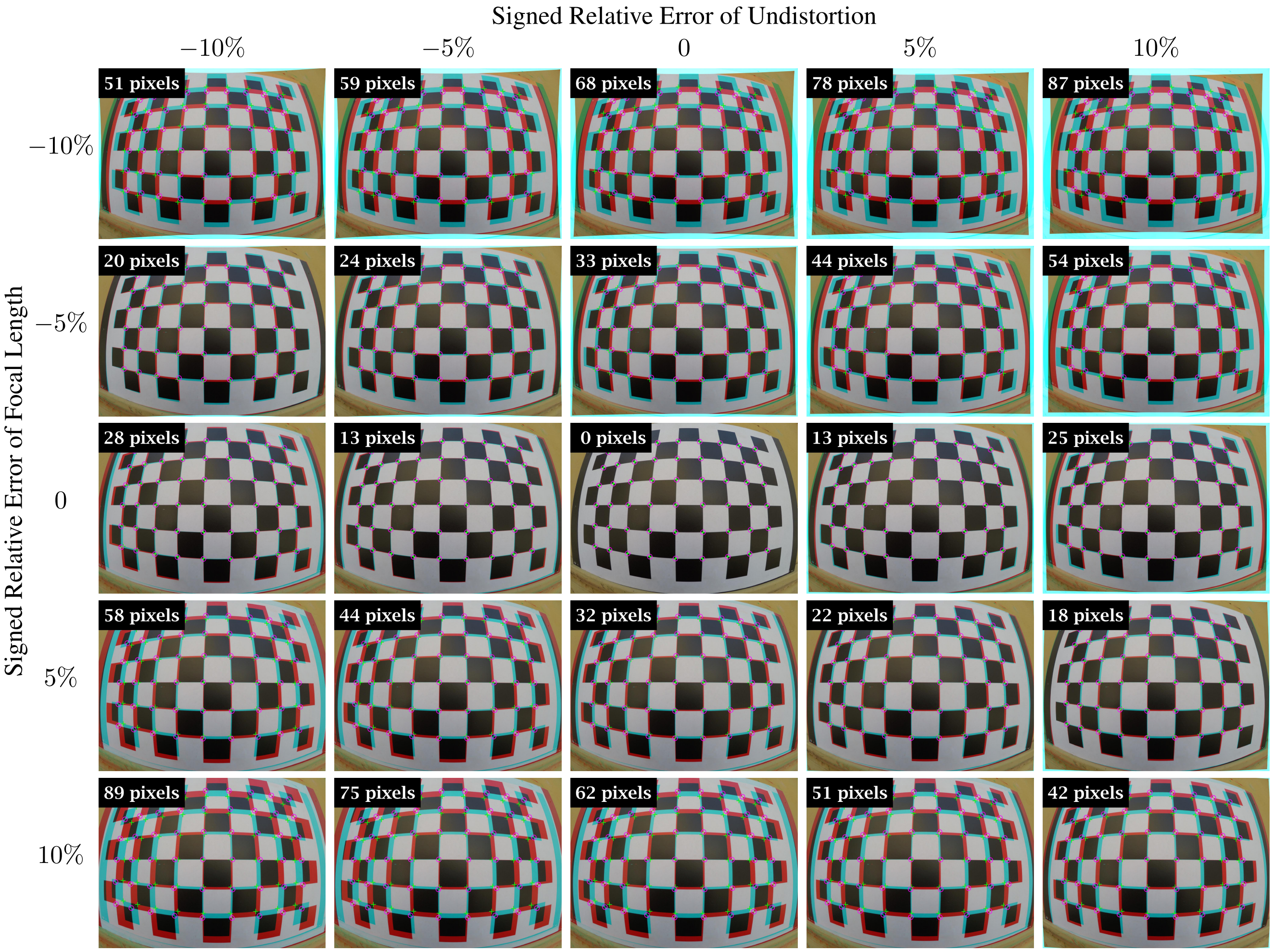

Table A.1: *Intrinsics Error vs. Warp Error.* Each cell is the composite image of the original image with its red channel subtracted and the re-warped image with only its red channel. The RMS warp error computed for a combination of relative error levels of focal length and division-model parameter is rendered in the top left corner of each image. Errors from perturbed intrinsics are visible as false colors in the composite images, which highlight bad registrations between the original and re-warped images. The input image resolution is 3000×2250 pixels.

B. Relating Warp Error and Intrinsics

The warp error introduced in Sec. 6.1 jointly captures errors in the estimates of the focal length f and the division model parameter of lens undistortion λ. Fig. A.3 and Table A.1 show the relation between the errors in the estimates of intrinsics parameters and the warp error. Fig. A.3 shows that the warp error is nonlinear, nonsymmetric function of the intrinsic relative errors. An error in focal length can be compensated by an error in undistortion and vice-versa.

The chessboard images in Table A.1 give geometric intuition of how the metric warp error Δ^{RMS} corresponds to registration errors between the original image and the re-warped image as synthesized according to Sec. 6.1. The images confirm an observation that the warp error is not proportional in its arguments. *E.g.* 10% relative error of undistortion with no error in focal length results in 25 pixels Δ^{RMS} however increasing the relative error of focal length to 5% will give 18 pixels Δ^{RMS} which means that the algebraic errors partially compensate each other leading to the lower geometric error.

C. Additional Synthetic Experiments

Fig. C.1 reports the cumulative distributions of the relative errors of undistortion and the relative errors of focal length for the individual solvers, the combination of all solvers, and the **6CA** & **2PC+4CA** combination.

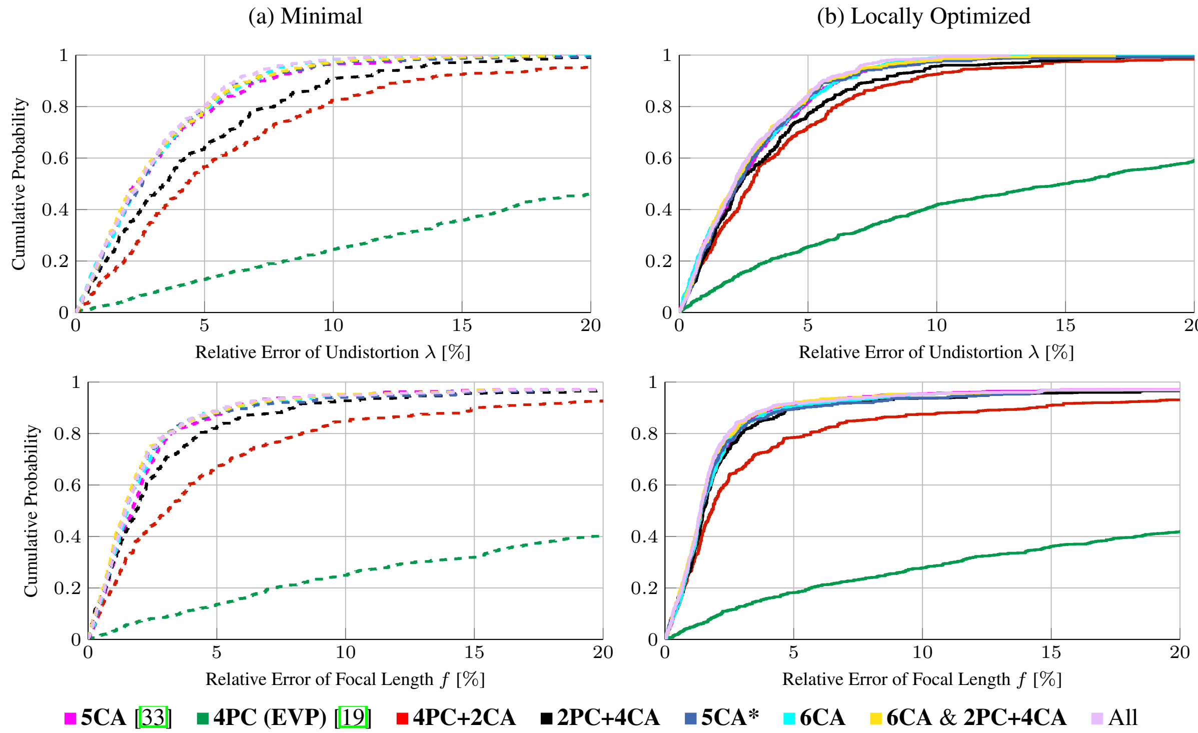

Figure C.1: Cumulative distributions of the relative error of the division model parameter λ and the relative error of the focal length f on AIT dataset [33]. Results are shown for (a) the minimal *i.e.* initial solutions and (b) locally optimized *i.e.* final solutions.

D. Additional Real-Image Experiments

Fig. D.1 provides qualitative results for the proposed solvers. The images were taken with four lenses mounted on Canon 5DSR camera: Sigma 8mm, Samayang 12mm, Sigma 15mm and Sigma 24mm. The solvers accurately calibrate cameras with fields of view from narrow to fisheye with diverse image content.

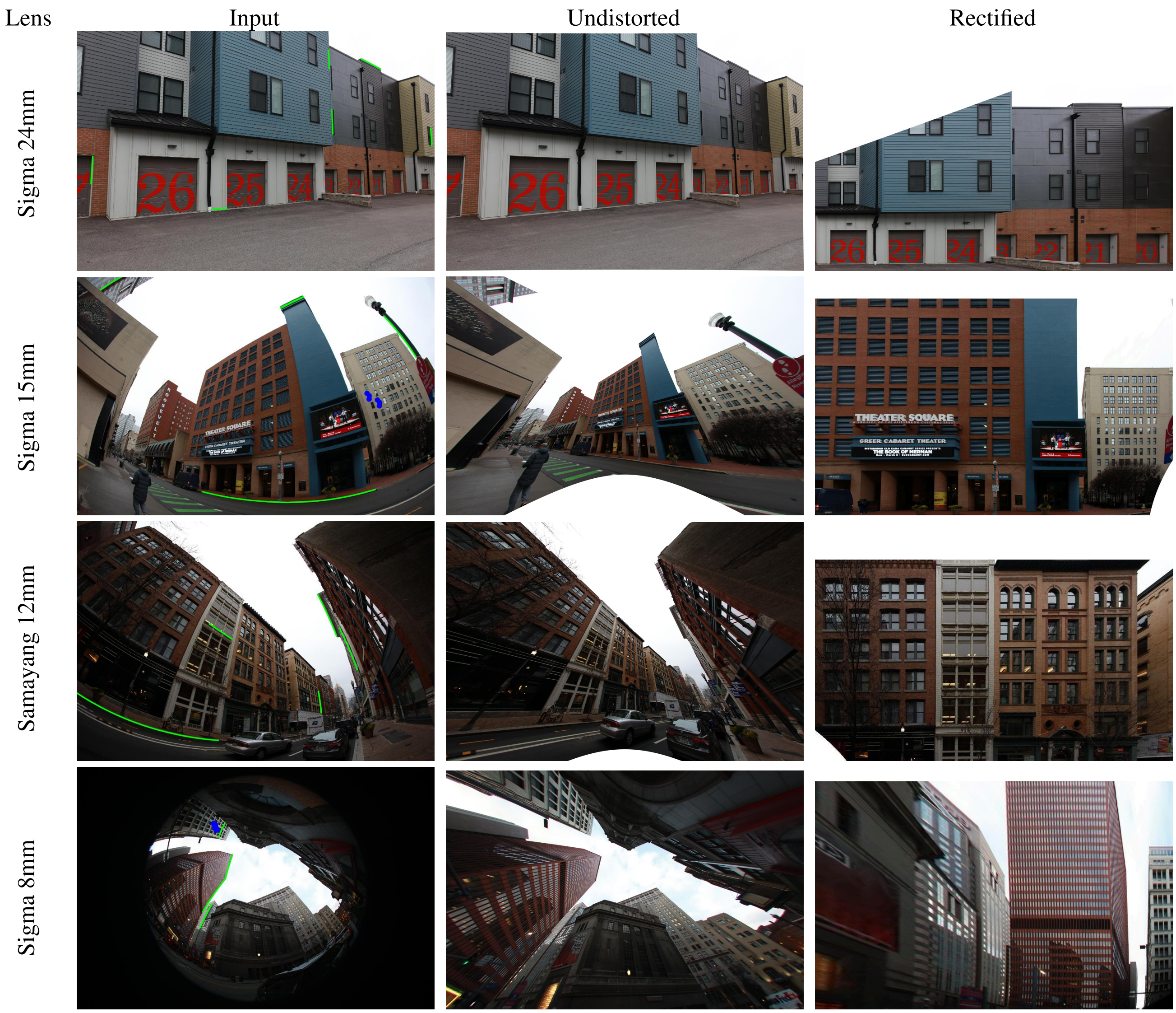

Figure D.1: *Field of View Study.* Auto-calibration results are shown for lenses with different fields of view from narrow to fisheye. The minimal sample —green circles and blue regions—of the returned solution is depicted on the input image.